Cerebral Cortex May 2009;19:1042-1054
doi:10.1093/cercor/bhn146
Advance Access publication September 11, 2008

Modulation of Ventral Prefrontal Cortex Functional Connections Reflects the Interplay of Cognitive Processes and Stimulus Characteristics

Andrea B. Protzner[1,2] and Anthony R. McIntosh[2,3]

[1]Toronto Western Hospital and Research Institute, Toronto, M5G 2M9 ON, Canada, [2]Department of Psychology, University of Toronto, Toronto, M5S 1A7 ON, Canada and [3]Rotman Research Institute of Baycrest Centre, Toronto, M6A 2E1 ON, Canada

Emerging ideas of brain function emphasize the context-dependency of regional contributions to cognitive operations, where the function of a particular region is constrained by its pattern of functional connectivity. We used functional magnetic resonance imaging to examine how modality of input (auditory or visual) affects prefrontal cortex (PFC) functional connectivity for simple working memory tasks. The hypothesis was that PFC would show contextually dependent changes in functional connectivity in relation to the modality of input despite similar cognitive demands. Participants were presented with auditory or visual bandpass-filtered noise stimuli, and performed 2 simple short-term memory tasks. Brain activation patterns independently mapped onto modality and task demands. Analysis of right ventral PFC functional connectivity, however, suggested these activity patterns interact. One functional connectivity pattern showed task differences independent of stimulus modality and involved ventromedial and dorsolateral prefrontal and occipitoparietal cortices. A second pattern showed task differences that varied with modality, engaging superior temporal and occipital association regions. Importantly, these association regions showed nonzero functional connectivity in all conditions, rather than showing a zero connectivity in one modality and nonzero in the other. These results underscore the interactive nature of brain processing, where modality-specific and process-specific networks interact for normal cognitive operations.

Keywords: audition, functional MRI, neural context, prefrontal cortex, vision

Introduction

Previous research has shown that functional connectivity, as measured by the covariance of activity between brain regions, changes when participants perform tasks that engage different cognitive processes (Horwitz et al. 1992; Friston 1994). Such data have been used to establish the notion of neural context, wherein the response properties of one element in a network are profoundly affected by the status of other neural elements in that network. As a result, the functional relevance of a given neural element will depend on the status of other interacting elements (Bressler and McIntosh 2007). For example, a functional magnetic resonance imaging (fMRI) study by Lenartowicz and McIntosh (2005) suggests that the anterior cingulate (ACC) can contribute to both memory and attentional processes when there are changes in the brain regions with which the ACC interacts. Participants performed a standard version of a 2-back working memory task with strong attentional demands, and a cued version that promoted memory retrieval. Although both tasks activated the ACC, its functional connections, and the relation of these connectivity patterns to memory performance were completely different in the 2 tasks. Therefore, the contribution of the ACC to memory- and attention-driven tasks was determined by other coactive brain regions. Another study of ACC functional connectivity (Stephan et al. 2003) used fMRI to examine whether hemispheric functional asymmetry was determined by a word stimulus (short words, with one letter colored red) or by the task. In one instance, subjects judged whether the word contained the letter "A," ignoring the red letter, and in another instance, they made a visuospatial judgment indicating whether the red letter was right or left of center. A direct comparison of brain activity revealed strong hemispheric differences. The letter task produced higher activity in the left hemisphere, whereas the visuospatial task produced higher activity in the right hemisphere. The ACC was similarly active in both tasks relative to baseline, but showed distinctly different patterns of functional connectivity between tasks. Specifically, during the letter task, the ACC was coupled to the left prefrontal cortex (PFC); during the visuospatial task, the ACC was linked with the right posterior parietal cortex. These data are a compelling example of how task demands can modulate the neural context within which a cortical area (i.e., the ACC) operates. Similar task-dependent functional connectivity patterns have been reported for the medial temporal lobe (McIntosh et al. 2003) and for middle PFC (McIntosh et al. 1997).

In the current study, we were interested in whether or not PFC functional connectivity varies for simple working memory tasks when the stimuli are presented through different modalities. We chose the PFC as our region of interest (ROI) because it is central for a wide variety of psychological processes, including attention, memory, and response selection. For example, dorsolateral regions are engaged in sustained attention (Stuss et al. 1995; Corbetta 1998). Middle and inferior regions are engaged in memory retrieval (Stuss et al. 1995; Nyberg 1998; Grady 1999). Lateral PFC is divided into dorsal/ventral steams by the working memory literature, and is related to either spatial versus nonspatial information (Wilson et al. 1993) or maintenance versus manipulation of stored information (Petrides 1994; Owen et al. 1996). Ventral and orbital PFC are involved in the use of conditional rules to select a course of action (Rushworth et al. 2005). Framed in the context of network operations, the strong involvement of PFC in attention, memory and response selection arises because it is well situated, in an anatomical sense, to establish the neural context of these processes. Its anatomical connections allow it to integrate information from distributed sensory and motor networks (Fuster 1997). The idea that a distributed pattern of activity across several regions differentiates attentional and

memory processes better than activity in any single region receives support from the existence of functional overlap within the PFC. For example, sustained attention, working memory, and verbal retrieval all engage middle PFC (Cabeza and Nyberg 2000).

Although there are no previous studies that examine modality-based differences in PFC functional connectivity using analogous tasks, there are studies that show input modality-based dissociations in the PFC. For example, Bushara et al. (1999) measured brain activity with PET while participants performed auditory and visual spatial localization tasks. The auditory stimuli were synthesized band-passed bursts with spectral and binaural localization cues. The visual stimuli were peripherally located flashing light emitting diodes. Bushara et al. found modality-specific areas in the superior parietal lobule, middle temporal, and lateral PFC. Crottaz-Herbette et al. (2004) used fMRI to explore modality-based differences in verbal and written numbers in a working memory task. They found increased activation in the left posterior parietal cortex during the visual verbal working memory task, and increased activation in the left dorsolateral PFC the auditory verbal working memory task. Both these studies identified small but significant modality-based dissociations in the PFC. However, they may have underestimated input modality-based dissociations in the PFC because in both cases, the stimuli could be translated into semantic representations that are not linked to input modality (i.e., a location in personal space for Bushara et al.'s study, and numbers for Crottaz-Herbette et al.'s study).

We examined input modality and task demand effects on PFC functional connectivity with simple working memory tasks using semantically devoid stimuli. We constructed matrices of one-dimensional band-pass filtered noise and presented them auditorily as noise bursts or visually as images (Protzner and McIntosh 2007). Psychophysical work by Visscher et al. (2007) suggests that auditory and visual representations of stimuli akin to ours undergo very similar transformations when they are encoded and retrieved from memory. Participants performed 4 experimental tasks (auditory temporal sequencing, visual temporal sequencing, auditory comparison, and visual comparison) and 2 control tasks (auditory control and visual control). These tasks were as similar as possible between modality, allowing us to look at the effect of input modality on neural network organization. Within modality, the inclusion of multiple tasks allowed us to examine the effect of performance strategy. Comparison tasks were designed to require maintenance and manipulation in working memory. Temporal sequencing tasks were designed to require maintenance of information in working memory. Although the comparison and temporal sequencing tasks have different attentional demands, task difficulty as measured by accuracy, was equated using psychophysical thresholds. Control tasks required neither maintenance nor manipulation because participants were not asked to compare the stimuli for task performance.

Within the PFC, we chose our ROI statistically. We used task spatiotemporal partial least squares (task PLS, McIntosh et al. 2004) to identify the PFC voxel whose activity most reliably differentiated experimental from control tasks. This voxel was located in the right inferior frontal gyrus, Brodmann's area (BA) 47 (Montreal Neurological Institute [MNI] coordinate: 44, 32, –12; see circled region in Fig. 3*A* for approximate seed location). Meta-analyses and review papers of working memory have suggested that ventral PFC, including BA 47, tends to be recruited for maintenance operations (Courtney et al. 1998; D'Esposito et al. 1998; Wager and Smith 2003) which would be a common processing demand for both the temporal sequencing and comparison tasks. We used seed spatiotemporal PLS (seed PLS) to examine the functional connectivity of this prefrontal seed. With this usage of PLS, we analyzed how BA 47 activity correlated across participants with the rest of the brain. PLS can sort the correlations into what is similar, and what is different across tasks. This seed PLS was conducted only on experimental tasks. The control tasks were not included to focus the analysis on the potential dependence of functional connectivity on the varying experimenter manipulated cognitive challenges and modality.

When tasks and stimuli presented in different modalities differ both physically and semantically, they enlist different neural networks. When *the same* tasks and stimuli are presented through different modalities, several possibilities exist for neural network organization. Seed PLS could identify 1) functional connections that are common for all experimental tasks, 2) functional connections that differentiate task demands (i.e., temporal sequencing tasks vs. comparison tasks), 3) functional connections that differentiate input modality (i.e., auditory versus visual tasks), and 4) functional connections that show an interaction between task demands and modality. The most interesting outcome would be the interaction between task demands and modality because it would indicate that functional network configuration is dependent on both task demands and input modality.

Materials and Methods

Participants

The experimental design has been described in detail in another paper (Protzner and McIntosh 2007). Briefly, seventeen participants took part in the study. Data from 5 participants were excluded because of improper task performance or technical difficulties. Data from the 12 remaining participants (6 males; mean age 27.4 years, range 20–36 years) were used in the analyses. All were right handed, reported no history of major medical, neurological or psychiatric disorders, normal hearing, and normal or corrected to normal vision. All participants gave informed consent in accordance with the Institutional Review Board of University of Toronto and Baycrest Centre.

Procedure

Each participant performed the following experimental tasks: auditory temporal sequencing, auditory comparison, visual temporal sequencing, and visual comparison with bandpass-filtered white noise stimuli. In the auditory conditions, the noise stimuli were played as sound bursts. In the visual conditions, the noise stimuli were displayed as visual textures. These tasks were as similar as possible between modality, and as different as possible within modality (given the constraint that we used identical stimulus presentations for each task). On the day of scanning, observers also performed an auditory and a visual control task.

In each experimental trial, 3 noise stimuli appeared successively for 500 ms, with a blank (silent/gray) interstimulus interval (ISI) of 500 ms. The center frequency of the bandpass filter differed for each stimulus. After the onset of the third stimulus, participants pressed one of 3 response keys to indicate their response. For auditory temporal sequencing, participants indicated when the tone with the highest pitch sounded: first, second, or third. For auditory comparison, participants compared the third sound to the first 2 sounds. They indicated if the third sound was lower, intermediate, or higher in pitch as compared to the first 2 sounds. For visual temporal sequencing, participants indicated when the visual texture with the highest spatial

frequencies appeared. For visual comparison, participants compared the last texture to the first 2 textures. They indicated whether the last texture's spatial frequency content was lower, intermediate, or higher than the first 2 textures. Control trials were identical to experimental trials, except that the center frequency of the bandpass filter was the same for all 3 stimuli, and participants pressed all 3 response buttons after the third stimulus was presented. On the day of scanning, the intertrial interval was chosen pseudorandomly, and lasted 3, 5, 7, 9, or 11 s. Specifically, each trial type had an identical distribution of intertrial interval (ITI) lengths, but the order of ITI lengths was chosen randomly. This ensured minimal contamination of the average blood oxygen level–dependent (BOLD) response for a trial type with preceding trials (see below for specifics of fMRI analysis).

Experimental participation took place across 4 days. To reduce potential learning effects and to obtain a stable threshold, all participants performed the tasks outside of the scanner on the first 3 days of testing. Based on the data collected, psychometric functions for center frequency ratio were determined (see stimulus description below), and 80% correct thresholds were estimated from best fitting Weibull curves using the QUEST adaptive staircase procedure (Watson and Pelli 1983; Press et al. 1989). On the day of scanning, each participant performed 40 trials of each experimental task as well as 40 trials of each control task. The trials were presented in 4 runs, with 2 blocks of 5 trials of each task. Blocks within runs were presented in random order across participants. Before each block, participants were presented with an instruction image indicating which task they would perform next, and which response the first response key indicated.

Stimuli

The visual stimuli were generated by filtering one-dimensional Gaussian white noise fields with a 2-octave frequency filter. During each trial, 3 textures appeared, differing in center frequency. The base frequency was jittered around 2 cycles per degree (cpd) by plus or minus 20%. The remaining 2 center frequencies increased by a constant ratio (e.g., at a ratio of 2, and a base frequency of 2 cpd the center frequencies were 2, 4, and 8 cpd). Task difficulty could be increased by decreasing the center frequency ratio. The order of presentation for the textures was chosen randomly. Each texture was 256 by 256 pixels in size, and was generated randomly. Peak Michelson contrast was 38%, and was modulated with a 2-dimensional Gaussian envelope. The average luminance of the stimulus was 15 cd/m^2. The background was gray with a luminance of 15 cd/m^2. Finally, the display was gray during the ISI, and had a luminance of 15 cd/m^2.

The auditory stimuli were generated and presented in the same manner as the visual stimuli, except that the 500-ms stimulus presentation included a rise and decay of 50 ms, and the base frequency was jittered around 600 Hz. The stimuli were presented at a sound level that was identified as comfortable by the participant at the beginning of each experimental session (e.g., approximately 80 dB sound pressure level).

Apparatus

A MacIntosh iBook (Apple Computers, Cupertino, CA) controlled stimulus presentation and response recording. On the first 2 days of testing, participants viewed the stimuli binocularly on the iBook's monitor, or listened to the stimuli presented through the iBook's speakers binaurally from a comfortable distance. Participants indicated their responses by pressing one of 3 specified keys (F, J, or K) on the iBook's keyboard. The experiment took place in a dimly lit, quiet room. On the third day, participants performed the tasks in an MRI simulator. Visual stimuli were projected using a Boxlight 6000 projector (Boxlight, Poulsbo, WA) onto a rear-projection screen, and viewed by the participants through a mirror mounted in the simulator's headcoil. Auditory stimuli were delivered to the participant at a comfortable sound level by fMRI compatible, acoustically padded headphones (Avotech, Jensen Beach, FL). Participants used their right index, middle, or ring fingers to indicate their responses on a Lumitouch Reply System response box (Lightwave Medical Industries, Burnaby, BC, Canada). On the fourth day, participants performed the tasks during fMRI acquisition. Stimulus presentation and response recording was performed in the same manner as in the MRI simulator.

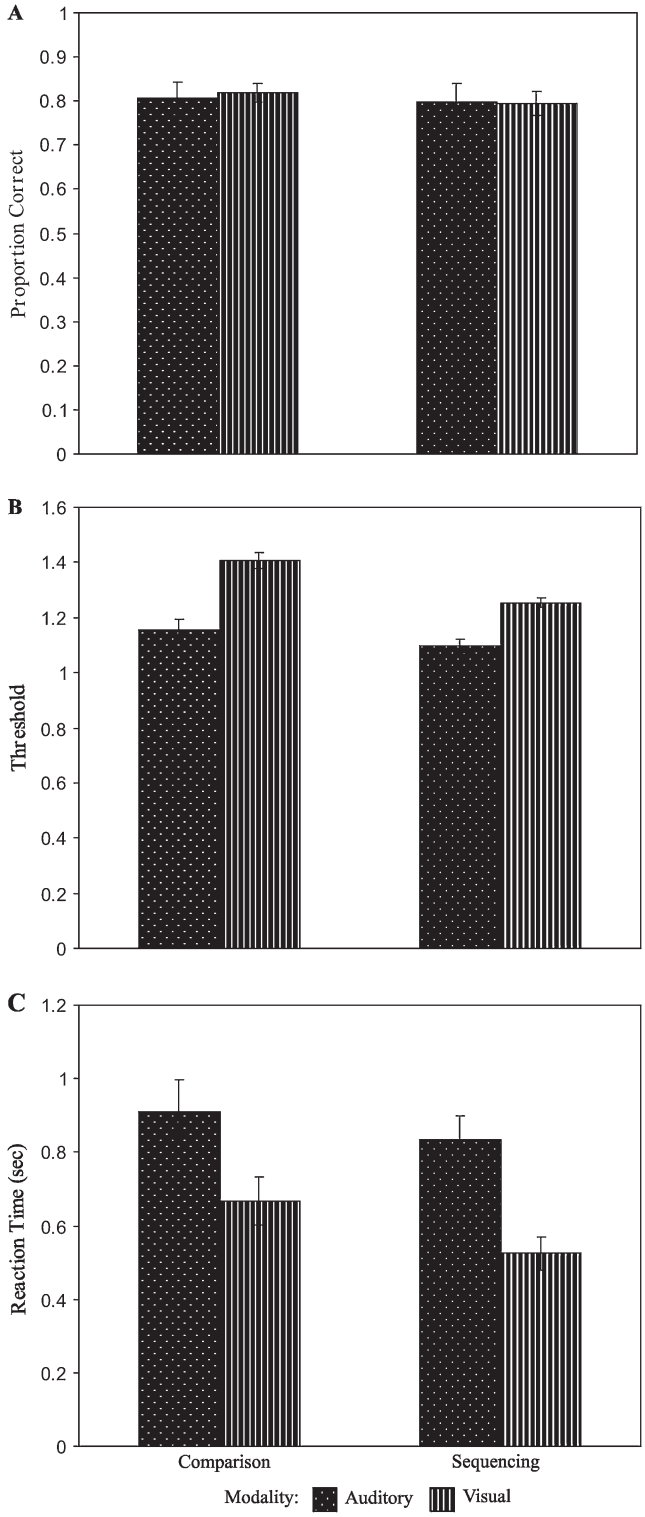

Figure 1. Behavior measures for the 4 experimental tasks. (*A*) Mean proportion correct. (*B*) Mean threshold. (*C*) Mean reaction time. Error bars show standard error.

fMRI Procedure

Regional cerebral activity was measured using a 1.5T Signa MR scanner with a standard quadrature headcoil (CV/I hardware, LX8.3 software: General Electric Medical Systems, Waukesha, WI). For each participant, a structural MRI was obtained by using a 3D T1-weighted pulse sequence (time repetition [TR] = 12.4 ms, time echo [TE] = 5.4 ms, flip

angle 35°, 22 × 16.5 field of view, 256 × 192 acquisition matrix, 124 axial slices 1.4 mm thick). Functional imaging measured brain activation by means of the BOLD effect with optimal signal contrast. Eighteen axial slices were acquired, each with a thickness of 7 mm. Functional scans were obtained using a single shot T_2^*-weighted pulse sequence with spiral readout, offline gridding, and reconstruction (TR = 2000 ms, TE = 40 ms, flip angle 80°, 90 × 90 effective acquisition matrix).

Data processing was performed using Analysis of Functional NeuroImaging software (http://afni.nimh.nih.gov/, Cox 1996). Time series data were spatially coregistered to correct for head motion by using a 3D Fourier transform interpolation. Motion-corrected images were then spatially transformed to an fMRI spiral scan template generated from 30 participants scanned locally. This template was registered to the MNI305 template. The transformation of each participant to the spiral template was achieved using a 12-parameter affine transform with sinc interpolation as implemented in SPM99 (http://www.fil.ion.ucl.ac.uk/spm/, Friston et al. 1995). Images were smoothed with an 8-mm isotropic Gaussian filter before analysis. For each participant, "brain" voxels in a specific image were defined as voxels with an intensity greater than 15% of the maximum value in that image. The union of masks was used for group analyses as described below.

Data Analysis

The primary image analysis was done with spatiotemporal PLS (McIntosh et al. 2004), a multivariate method that enables the identification of the optimal spatial and temporal patterns that either differentiate tasks in terms of activation, or in terms of functional connectivity. PLS operates on the entire data structure at once, which requires that the data be in matrix form. The rows of the data matrix are arranged as follows; condition blocks are stacked and each participant has a row of data within each condition block. With *n*

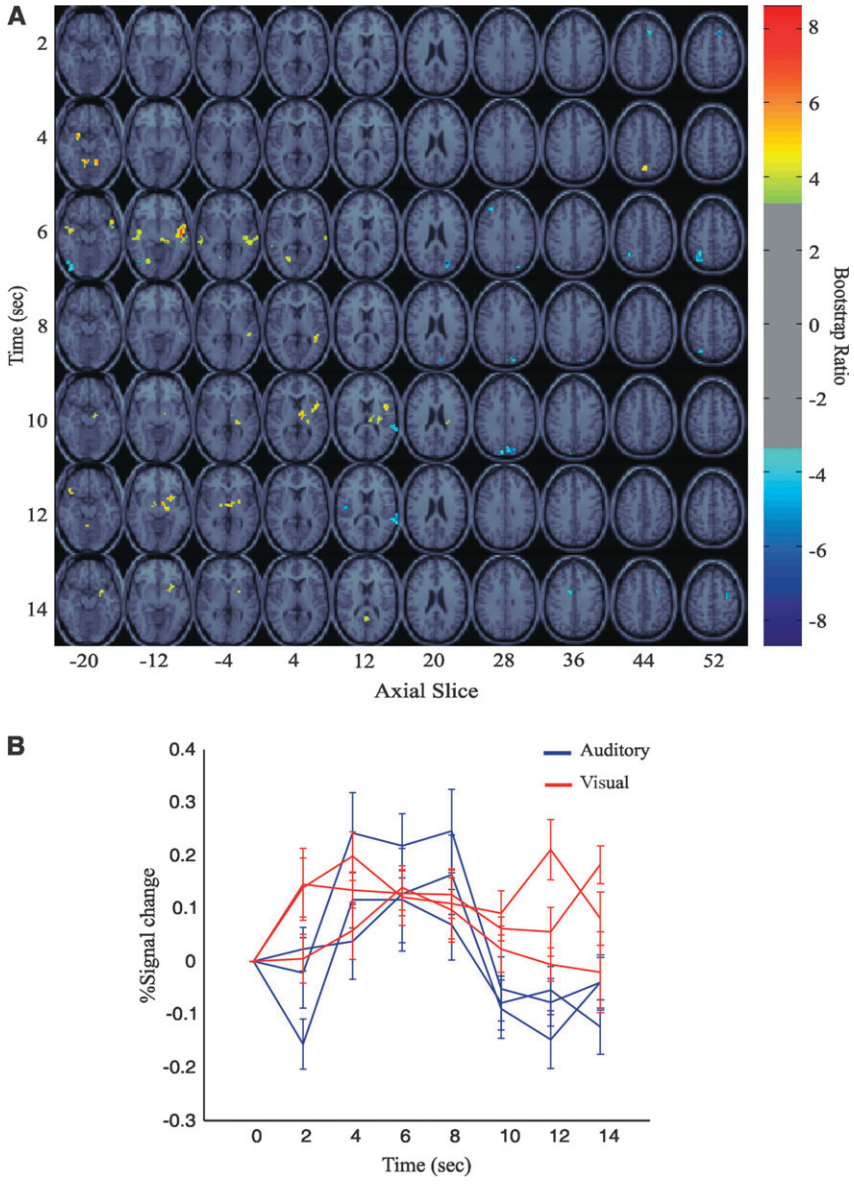

Figure 2. (*A*) Singular image for the nonrotated task PLS modality LV. On the singular image, time from stimulus onset, expressed in seconds, is indicated on the *y*-axis of the singular image. The approximate location of the axial slice in MNI atlas space is indicated on the *x*-axis. Voxels in the image are highlighted according to the magnitude of the ratio of their parameter estimate to the bootstrap-estimated standard error (bootstrap ratio). The singular image is superimposed on a T_1-weighted MRI template. On the singular image, brain regions in blue are more active during visual tasks, and brain regions in yellow are more active during auditory tasks. (*B*) HRF from BA 22, identified in the modality LV as more active during the visual tasks (MNI template coordinates: $x = 68$, $y = -40$, $z = 12$). Auditory tasks are shown in blue and visual in red to emphasize that change in response was greater for auditory than visual tasks. Responses are expressed as percent change from stimulus onset ($T = 0$) and are averaged across subjects (±SE).

Table 1
Local maxima from the nonrotated task PLS

Lag	*x* (mm)	*y* (mm)	*z* (mm)	BSR	Cluster size (voxels)	Region
Modality LV						
2	8	−28	−28	5.4523	25	Colliculus
2	−52	16	−36	4.8237	15	GTs (BA 38)
2	12	24	48	−7.0958	18	GFd (BA 8)
4	−8	−52	−20	6.8221	18	Cerebellum
4	16	−52	−24	5.9915	15	Cerebellum
4	4	−64	48	5.8111	23	PCu (BA 7)
4	−24	0	−16	5.8033	14	NA (BA 34)
6	52	0	−16	7.3127	180	GTm (BA 21)
6	−24	−68	−16	7.2975	16	GF (BA 19)
6	20	−28	−12	5.9648	19	GH (BA 28/35)
6	−44	−8	−20	5.5354	95	GTm (BA 21)
6	−28	−64	4	4.1564	18	GOm (BA 19/37)
6	24	−76	20	−8.7074	28	GOm (BA 18)
6	−36	40	24	−6.0116	15	GFm (BA 46)
6	−36	−60	52	−5.5633	85	LPs (BA 7)
6	−52	−76	−28	−4.492	49	Cerebellum
8	40	−44	4	5.4865	41	GTm (BA 22)
8	−28	−72	60	−6.1066	58	LPs (BA 7)
8	28	−36	−32	−6.0643	23	Cerebellum
10	8	−12	4	6.5954	81	Thalamus
10	44	8	8	6.2065	45	GPrC (BA 6)
10	24	−28	0	5.5604	41	Pulvinar
10	16	−16	−16	5.3766	16	Midbrain
10	−12	−96	28	−8.1526	20	Cu (BA 19)
10	12	−84	28	−5.9613	57	Cu (BA 19)
12	24	4	−12	6.2036	37	Caudate
12	4	−8	−4	6.1644	72	Ventromedial thalamus
12	−40	20	−28	5.359	24	GTs (BA 38)
12	68	−40	12	−5.6058	31	GTs (BA 22)
12	−48	−8	8	−5.0095	30	GTs (BA 22)
14	0	−56	12	4.0285	20	GC (BA 23/30)
14	−12	−4	32	−5.572	12	GC (BA 24)
14	32	−4	52	−5.0262	16	GFm (BA 6)
Task demands LV						
2	8	32	48	5.1218	16	GFd (BA 8)
4	−32	−64	−8	6.015	19	GL (BA 19)
4	−36	−52	−44	−5.993	18	Cerebellum
6	−28	−64	−44	7.2923	29	Cerebellum
6	68	−28	8	4.8578	30	GTs (BA 42)
6	52	−68	−20	4.1104	15	GF (BA 19/37)
6	28	56	28	−5.7642	13	GFs (BA 10)
6	−48	−68	32	−5.2	17	Ga (BA 39)
6	−60	−48	−16	−5.0959	12	GTi (BA 37)
6	−24	56	24	−4.8641	11	GFs (BA 10)
6	0	−48	32	−4.1364	19	PCu (BA 7)
8	−4	8	52	7.7086	90	GFd (BA 6)
8	−32	20	4	5.9997	15	Insula
8	12	−72	56	5.7997	37	LPs (BA 7)
8	−28	−64	36	5.5719	97	Ga (BA 39)
8	24	−8	60	5.3013	20	GFm (BA 6)
8	36	−52	52	4.6394	37	LPi (BA 40)
8	−60	−8	44	4.6054	17	GPrC (BA 6)
8	36	16	0	4.3895	17	GFm (BA 9)
8	8	−28	0	4.2658	14	Th
8	40	4	24	4.0916	13	GPrC (BA 4)
8	12	12	−8	4.0004	20	NC
8	16	56	40	−7.1003	26	GFs (BA 9)
8	−8	44	44	−5.8488	13	GFd (BA 8)
8	−4	56	4	−5.3611	103	GFd (BA 10)
8	−36	24	36	−5.0967	35	GFm (BA 9)
8	−24	44	36	−5.0848	11	GFs (BA 9)
8	4	−48	28	−4.7719	19	GC (BA 31)
8	4	44	56	−4.6957	14	GFs (BA 8)
8	0	28	0	−4.5363	15	NC
8	0	−24	44	−4.4405	12	GC (BA 31)
10	12	−52	−12	6.3035	40	Cerebellar vermis
10	44	−4	−36	6.0853	13	GTm (BA 21)
10	−20	32	−4	−9.6241	31	GC (BA 24)
10	0	−40	68	−6.6705	55	LPc (BA 4)
10	68	−16	8	−5.6468	13	GTs (BA 22)
10	8	40	0	−4.3109	12	GC (BA 32)
12	44	32	−24	9.2229	22	GFi (BA 47)
12	36	0	−24	6.0269	22	NA
12	24	4	4	5.1794	42	NL
12	52	−60	20	4.9644	18	LPi (BA 39)
12	−20	−76	52	−8.2086	28	PCu (BA 7)
12	−16	4	60	−7.5884	39	GFd (BA 6)
12	−48	8	36	−6.7087	24	GFi (BA 44)
12	56	8	36	−5.6659	16	GFi (BA 44)
12	−28	4	56	−5.5023	28	GFm (BA 6)
14	−44	−52	12	6.673	14	GTs (BA 22)
14	56	−64	36	6.1539	31	Ga (BA 39)
14	−56	−64	20	5.0206	18	LPi (BA 39)
14	28	−80	−20	4.4941	11	GF (BA 18)
14	−40	56	16	−6.5099	46	GFm (BA 10)
14	−40	28	20	−5.7566	15	GFi (BA 45)
14	8	−72	48	−5.5128	31	PCu (BA 7)
14	−52	4	24	−5.0636	29	GPrC (BA 6)

Note: Lag refers to the period, in seconds, after stimulus onset during which the peak occurred. *x*, *y*, and *z* indicate voxel coordinates in MNI space. BSR represents each voxel's PLS parameter estimate divided by its standard error. Cluster size refers to the number of contiguous voxels included in the cluster. Regions indicate the gyral locations and BA of the cluster peak. MNI coordinates were converted into Talairach coordinates using the *mni2tal* script (http://eeg.sourceforge.net/mridoc/mri_toolbox/mni2tal.html). Gyral locations and BA were then determined by reference to Talairach and Tournoux (1988).

participants and k conditions, there are $n \times k$ rows in the matrix. The columns of the data matrix contain the signal intensity measure for each voxel at each time point. The first column has intensity for the first voxel at the first time point, the second column has the intensity for the first voxel at the second time point. With m voxels and t time points, there are $m \times t$ columns in the matrix. The hemodynamic response function (HRF) for any given condition normally lasts for several scans; thus, a "lag window" is defined for as a short signal segment within a trial that represents the response of each voxel. In the current experiment, the lag-window size was 8 (TR = 2, 16 s), beginning at the onset of each trial. The HRF for each trial is expressed as the intensity difference from trial onset.

Two forms of PLS were performed. The first, nonrotated task PLS, assessed whether there were differences between groups in task-dependent brain activity. This analysis also allowed us to identify a seed voxel whose activity differentiated task demands, located in BA 47. The second, seed PLS, identified cortical regions that were functionally connected with the BA 47 voxel. These analyses are explained further below.

Nonrotated Task PLS

Task PLS is able to identify time-varying distributed activity patterns, or latent variables (LVs), that differentiate experimental conditions. Usually, task PLS uses singular value decomposition to rotate the data matrix to identify the strongest effects in the data. We used a nonrotated version of task PLS, in which a priori contrasts restrict the patterns derived from task PLS (McIntosh and Lobaugh 2004). The effects of interest were a main effect of modality (i.e., auditory vs. visual), a main effect of task demands, and an interaction between modality and task demands. A "singular image" is computed for each contrast representing the distributed voxel pattern that embodies the effect. The strength of the relationship between the singular image and the contrast is given by the singular value. For the nonrotated task PLS, the singular image is simply the cross product of a contrast and the data matrix and the singular value is the sum of squared voxel values for the singular image. This version of task PLS has the advantage of allowing a direct assessment of hypothesized experimental effects. There is, however, no guarantee that these effects are the strongest which can be identified using the original version of task PLS with singular value decomposition.

Statistical assessment for PLS is done using permutation tests for the LVs and bootstrap estimation of standard errors for the voxel saliences. The permutation test assesses whether the effect represented in a given LV, captured by the singular value, is sufficiently strong to be different from random noise. The standard error estimates of the voxel weights/saliences in each singular image from the bootstrap tests are used to assess the reliability of the nonzero saliences in significant LVs.

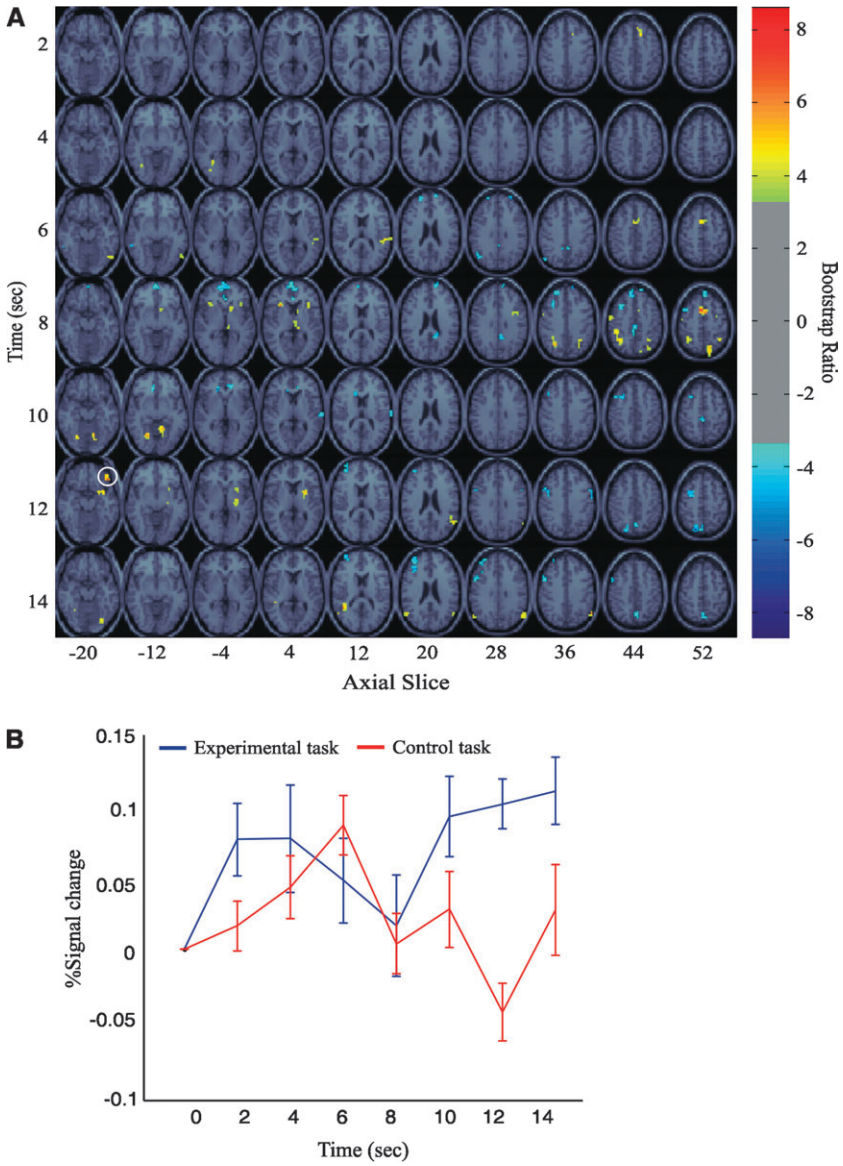

Figure 3. (*A*) Singular image for the nonrotated task PLS task demands LV. Brain regions in blue are more active during control tasks, and brain regions in yellow are more active during experimental tasks. White circle indicates the approximate location of the BA 47 seed voxel used in the seed PLS analysis. (*B*) Hemodynamic response function from the seed voxel circled in (*A*) (MNI template coordinates: $x = 44$, $y = 32$, $z = -24$). The averaged response for experimental tasks is shown in blue, and averaged response for control tasks are shown in red. Responses are expressed as percent change from stimulus onset ($T = 0$) and are averaged across subjects ($\pm$SE).

This ratio is proportional to a *z*-score, but should be interpreted as a confidence interval, where we designated a threshold of 3.3 corresponding roughly to a 99.9% confidence interval.

Seed PLS

Seed PLS examines the correlations between a seed ROI and the rest of the brain. Seed PLS identifies LV that capture task and group dependent changes in functional connectivity between the seed ROI and the rest of the brain (i.e., brain-seed correlations). It is conceptually similar to the univariate version of psychophysiological interactions that can be used to assess experimental-context dependent changes in functional connectivity (Friston et al. 1997). The correlation of the fMRI signal for the seed and for the rest of the brain is computed across participants within each task, resulting in a matrix of within-task brain-seed correlation maps. Singular value decomposition of the brain-seed correlation matrix produces 3 new matrices: the singular image of voxel saliences, singular values, and task saliences. The variation across the task saliences indicates whether a given LV represents a similarity or difference in the brain-seed correlation across tasks. This can also be shown by calculation of correlation between the brain scores (dot-product of the voxel salience and fMRI data) and seed fMRI signal for each task. The voxel saliences give the corresponding spatiotemporal activity pattern. Statistical assessment is similar to that used for task PLS.

Results

Behavioral Performance

Measures of reaction time, accuracy, and threshold are summarized in Figure 1. We performed a 2 (modality) × 2 (experimental tasks) repeated measures analysis of variance on reaction time, accuracy, and threshold data from the day of scanning. For percent correct data (see Fig. 1*A*), all effects were statistically nonsignificant, indicating that task difficulty, as indicated by response accuracy, was equated across all

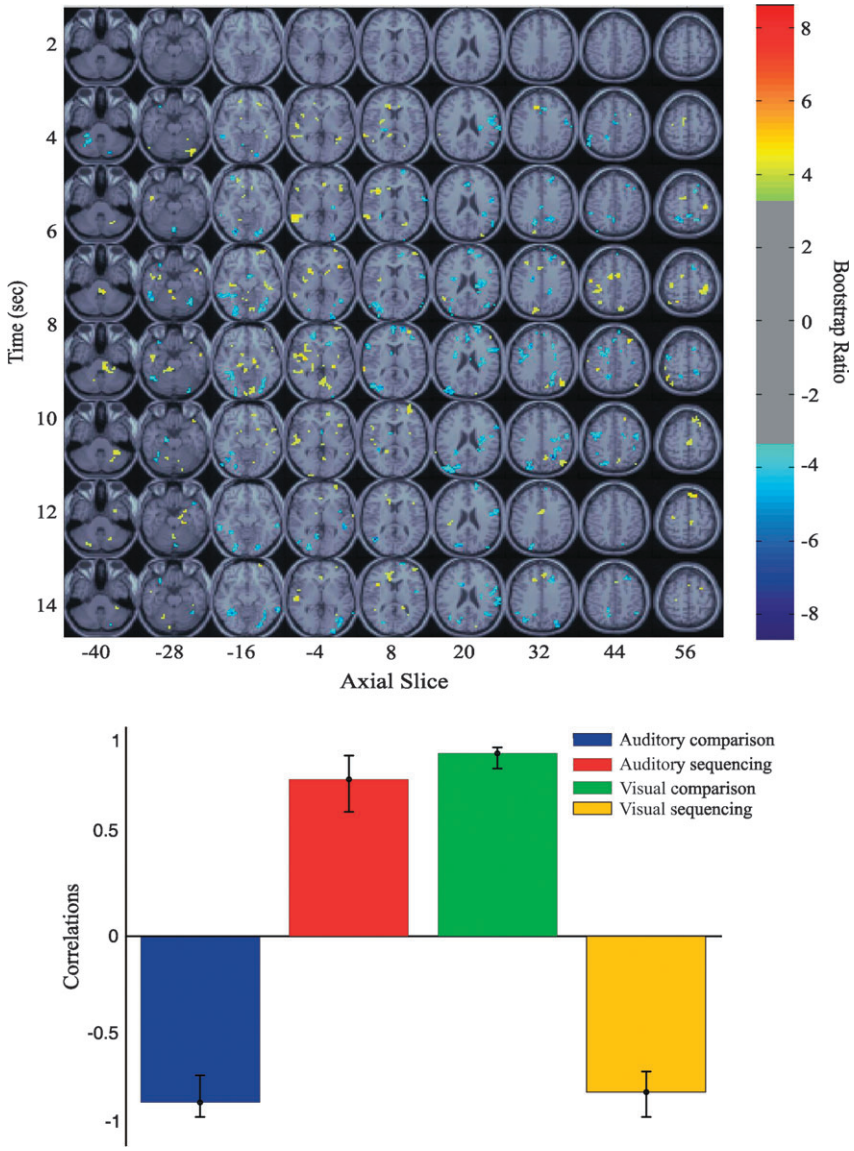

Figure 4. Singular image (top) and correlation between brain scores and the BA 47 seed voxel for the interaction LV from seed PLS. The singular image identifies peak voxels showing a different pattern of correlations with the BA 47 voxel across tasks. The correlation bar graph captures the task-dependent changes in the correlation with the seed voxel of the areas identified in the singular image. The error bars indicate the 95% confidence interval derived from bootstrap estimation.

experimental tasks. For threshold data (see Fig. 1*A*), the main effects of modality ($F_{1,11}$ = 36.40, P < 0.001) and task ($F_{1,11}$ = 41.59, P < 0.001) were significant. The main effect of modality indicates that auditory thresholds were generally lower than visual thresholds. The main effect of task indicates that comparison thresholds were generally higher than temporal sequencing thresholds. The interaction between modality and task also was significant ($F_{1,11}$ = 9.27, P < 0.05), indicating that the difference between comparison and temporal sequencing thresholds was bigger for visual than for auditory tasks. For reaction time data (see Fig. 1*A*), the main effects of modality ($F_{1,11}$ = 49.78, P < 0.001) and task ($F_{1,11}$ = 12.13, P < 0.01) were significant. The main effect of modality indicates that auditory tasks were performed with longer reaction times than visual tasks. Finally, the main effect of task indicates that comparison tasks were associated with longer reaction times than sequencing tasks. The interaction term was nonsignificant.

fMRI Results

Nonrotated PLS

The nonrotated task PLS was conducted with 3 contrasts: 2 for main effects and 1 interaction term. Statistical assessment identified both main effects as significant (modality LV singular value = 30.56, P < 0.001; task demands LV singular value = 28.14, P < 0.01), but the interaction term was nonsignificant (interaction LV singular value = 23.12, P = 0.162).

The LV that showed the strongest effect was the contrast between auditory and visual tasks (modality LV, Fig. 2*A*, see Table 1 for a list of local maxima). Dominant negative saliences (related to increased activation during visual tasks) were located in left middle frontal gyrus (BA 46), right medial frontal gyrus (BA 8), bilateral superior temporal gyrus (BA 22), left superior parietal lobe (BA 7), right cuneus (BA 19), and bilateral cerebellum. Dominant positive weights (related to increased

Table 2
Local maxima from the seed PLS

Lag	*x* (mm)	*y* (mm)	*z* (mm)	BSR	Cluster size (voxels)	Region
Interaction LV						
2	−8	−52	40	−6.5135	15	PCu (BA 7)
2	52	−8	32	−6.3323	29	GFi (BA 44)
2	−56	−56	44	−5.9159	17	LPi (BA 7/40)
2	−36	−60	−44	−5.3358	13	Cerebellar nucleus
2	36	−84	−32	5.4411	28	Cerebellum
2	−16	0	−12	6.5424	12	Ventral thalamus
4	−20	−56	56	−7.3346	23	PCu (BA 7)
4	24	−100	−4	−6.7995	14	GOm (BA 18)
4	12	−52	32	−6.0404	23	PCu (BA 19/31)
4	20	−88	−16	−5.5288	19	GL (BA 18)
4	−4	−48	36	−5.0515	11	PCu (BA 19/31)
4	−16	−60	32	−4.144	11	PCu (BA 19/31)
4	8	20	−12	5.9337	28	Caudate
4	−36	12	8	8.3526	29	GFi (BA 47)
4	−60	−48	0	14.219	71	GTm (BA 21)
6	−36	−100	16	−10.6274	49	GOm (BA 18)
6	40	−60	−12	−7.9156	25	GL (BA 19)
6	20	−100	0	−7.8276	23	GL (BA 18)
6	−52	−52	−28	−6.5618	42	GF (BA 37)
6	−32	28	−24	−5.482	11	GFi (BA 47)
6	4	24	64	−5.3652	11	GFd (BA 6)
6	−16	−80	28	5.5241	18	Cu (BA 19)
6	−44	−64	52	5.7818	24	LPs (BA 7)
6	−12	0	52	5.8066	30	GC (BA 24)
6	12	−84	48	6.0087	16	PCu (BA 7)
6	−36	−36	44	6.0831	11	LPi (BA 40)
6	−32	−8	8	6.5866	14	Insula
6	−36	28	36	6.7772	12	GFm (BA 9)
6	36	−32	56	6.8035	35	LPi (BA 40)
6	40	20	−4	8.3683	15	GFi (BA 47)
6	48	12	−28	9.6304	12	GFi (BA 47)
8	−40	−88	16	−8.8489	82	GL (BA 19)
8	16	64	4	−8.7088	53	GFs (BA 10)
8	−24	20	32	−6.8068	19	GFm (BA 9)
8	−44	−60	−24	−5.6193	34	GF (BA 37)
8	48	8	16	−5.524	28	GFi (BA 44)
8	4	48	36	−5.5045	12	GFd (BA 10)
8	−20	44	−8	−5.3603	13	GC (BA 32)
8	28	−84	−12	−5.2614	31	GL (BA 18)
8	−8	−32	−32	5.2443	25	Midbrain
8	−36	20	−12	5.3792	23	GFi (BA 47)
8	−20	−24	−8	5.5947	12	Pulvinar
8	8	−96	−20	5.6234	25	GL (BA 18)
8	8	−28	−36	5.772	20	Midbrain
8	40	−4	4	6.0159	14	GTs (BA 22)
8	32	32	44	6.1309	13	GFm (BA 8)
8	4	−64	−4	6.2584	13	GL (BA 19)
8	40	−68	32	6.6734	23	LPi (BA 40)
8	−36	−12	−8	7.2935	48	Putamen
10	−24	−72	40	−10.5928	27	LPi (BA 40)
10	−44	−12	40	−8.7358	29	GPrC (BA 6)
10	60	12	24	−7.0075	20	GFi (BA 44)
10	28	52	8	6.7585	16	GFs (BA 10)
Task demands LV						
2	44	−16	56	−7.7802	14	GPrC (BA 4/6)
2	40	−84	16	−7.0887	20	GOm (BA 18)
2	12	−32	−52	−5.1056	11	Pons
2	44	−28	24	5.407	21	LPi (BA 40)
2	0	60	−4	10.4845	154	GFs (BA 10)
4	32	−60	0	−8.3275	17	GL (BA 19)
4	16	−8	−32	−6.2251	14	GH (BA 28)
4	−4	28	28	−6.1385	11	GC (BA 32)
4	−60	−32	−12	4.7803	11	GTm (BA 21)
4	12	−48	48	5.3033	18	GC (BA 31)
4	−28	−12	4	5.4148	20	Putamen
4	−8	52	44	5.7221	19	GFd (BA 8)
4	−40	−36	0	6.4827	38	GTT (BA 42)
4	60	−20	−4	6.8219	44	GTT/GTs (BA 41)
4	12	−44	20	6.9448	16	GC (BA 23)
4	0	32	64	6.9457	18	GFs (BA 6/8)
6	−56	20	−24	−7.2603	32	GTs (BA 38)
6	28	−52	0	−5.8115	14	GL (BA 19)
6	−36	−80	−12	4.8746	11	GOm (BA 19/37)
6	−56	−20	40	5.1837	15	GPrC (BA 4/6)
6	−20	−16	−12	5.667	13	Midbrain
6	−56	−32	−8	5.9854	26	GTm (BA 21/22)
6	12	44	0	6.3428	23	GFs (BA 10)
6	60	−20	40	7.2913	31	GPrC (BA 4/6)
6	16	−12	12	7.7929	24	Thalamus
6	−52	−56	−8	7.9015	15	GTm (BA 21/37)
8	24	48	40	−6.8157	13	GFs (BA 9)
8	−28	48	−24	−6.1058	27	GFi (BA 11)
8	−4	20	−16	−5.5713	11	Gsc (BA 25)
8	−4	−20	0	4.9195	11	Thalamus
8	−44	−44	20	5.4323	12	LPi (BA 39/40)
8	−16	−68	40	5.4813	12	PCu (BA 19)
8	−36	−32	52	5.8544	30	GPoC (BA 4)
8	−48	−60	−8	6.2422	11	GTm (BA 21)
8	36	0	28	6.2908	13	GFi (BA 44)
8	−4	−32	20	6.723	32	GC (BA 23)
8	44	−48	48	7.1422	21	LPi (BA 40)
8	60	−8	36	8.8344	39	GPrC (BA 4/6)
10	20	−92	−4	−8.2562	16	GL (BA 17/18)
10	32	−36	60	−7.5726	33	LPs (BA 7/40)
10	−24	24	36	−5.8762	18	GFm (BA 9)
10	−8	56	20	−5.7708	11	GFd (BA 9)
10	32	−4	0	6.2581	16	Pons
10	−16	−56	32	6.9027	25	PCu (BA 7)
12	16	−96	24	−9.0107	44	GO (BA 19)
12	44	40	20	−8.9759	14	GFm (BA 46/9)
12	8	44	−20	−6.5604	13	GFd (BA 11)
12	−44	−80	28	−6.3583	51	GO (BA 19)
12	−4	24	32	−5.9349	12	GC (BA 32)
12	−40	52	−8	−5.7705	37	GFm (BA 10)
12	−12	−68	8	−5.6775	24	Cu (BA 31)
12	60	−60	16	−5.4906	27	GTm (BA 39)
12	−52	28	0	−5.1837	12	GFi (BA 45)
12	4	−36	68	5.0485	12	LPc (BA 5/7)
12	−48	−52	−16	5.7468	21	GTm (BA 37)
12	52	−20	8	5.8708	27	GTT (BA 41/42)
12	20	−16	12	6.2956	66	Pulvinar
12	4	−40	20	6.9112	106	GC (BA 29/30)
12	−40	−20	16	7.2314	49	GTT (BA 41/42)
12	44	4	4	7.3045	11	GTs (BA 22)
12	−28	−4	24	8.3192	38	Caudate
12	20	−72	44	8.5448	26	PCu (BA 7)
14	16	−84	20	−8.3323	36	GO (BA 19)
14	−24	−8	60	−8.2393	23	GPrC (BA 4/6)
14	−12	−76	4	−7.5163	42	GL (BA 18)
14	16	−76	−4	−6.5799	18	GL (BA 18)
14	−44	0	60	−6.2714	17	GPrC (BA 4/6)
14	−40	−80	20	−5.9341	23	GTm (BA 19)
14	32	56	−12	−5.0919	21	GFm (BA 10)
14	−40	52	20	−4.6846	11	GFm (BA 46)
14	−36	36	44	−4.5176	12	GFm (BA 8/9)
14	−28	−60	−36	4.6213	17	Cerebellum
14	−12	−32	12	6.2364	23	Pulvinar
14	−52	−28	−12	8.1038	28	GTm (BA 21)

Note: Lag refers to the period, in seconds, after stimulus onset during which the peak occurred. *x*, *y*, and *z* indicate voxel coordinates in MNI space. BSR represents each voxel's seed PLS parameter estimate divided by its standard error. Cluster size refers to the number of contiguous voxels included in the cluster. Regions indicate the gyral locations and BA of the cluster peak. MNI coordinates were converted into Talairach coordinates using the *mni2tal* script (http://eeg.sourceforge.net/mridoc/mri_toolbox/mni2tal.html). Gyral locations and BA were then determined by reference to Talairach and Tournoux (1988).

activation during auditory tasks) were located in right caudate, bilateral middle temporal cortex (BA 21b and 22r), right precentral gyrus (BA 6), and right thalamus.

Of note is the finding that saliences in the modality LV related to increased activation during the visual tasks include BA 22. This area typically is thought of as unimodal auditory cortex. It is not surprising that auditory sensory areas are activated during the visual tasks because the experiment was performed during fMRI scanning, which produces an acoustical artifact. However, one would still not expect BA 22 to be more active during the visual than auditory tasks. An examination of

the hemodynamic response function for this voxel (Fig. 2*B*) reveals that mean activation at the significant lags is greater during the visual tasks because this voxel is deactivating near the end of the lag window for auditory tasks. Therefore, there is greater *change* in activation for auditory conditions. The opposite pattern also occurs for auditory tasks. Saliences related to increased activation during the auditory tasks include BA 19, which is a region typically thought of as unimodal visual cortex. This area showed sustained activity across the entire temporal window for the auditory condition, but showed more modulation in visual conditions (data not shown). Again, it is not surprising that visual sensory areas are activated during the auditory tasks because participants are asked to fixate on a fixation cross during auditory task performance, and can see parts of the headcoil and the magnet bore. Importantly, the *change* in activation in unimodal visual areas is greater for visual tasks than auditory tasks.

The second significant LV was the contrast between experimental and control tasks (task demands LV, Fig. 3*A*, see Table 1 for a list of local maxima). Dominant negative weights (related to increased activation during control tasks) were located in left middle frontal gyrus (BA 9 and 10), left medial frontal gyrus (BA 6 and 10), left ACC (BA 24), right precuneus (BA 7), and paracentral lobule (BA 4). Dominant positive weights (related to increased activation experimental tasks) were located in left medial frontal gyrus (BA 6), right superior temporal gyrus (BA 42), right inferior frontal gyrus (BA 47), right lenticular nucleus, right superior parietal lobe (BA 7), right inferior parietal lobe (BA 40), bilateral angular gyrus (BA 39), and right cerebellar vermis. The right inferior frontal gyrus (BA 47) was used as the seed voxel for the seed PLS analysis described below. The hemodynamic response function for this voxel is displayed in Figure 3*B*, showing both early and late separation between experimental and control tasks.

Seed PLS

The seed PLS was conducted only for experimental tasks. The control tasks were not included to focus the analysis on the potential dependence of functional connectivity on experimenter manipulated variations in cognitive demands and modality. It should be emphasized that inclusion of the control task in the analysis did not change the pattern of results we report here.

Two significant patterns were identified by the seed PLS. The first depicted a task demand by modality interaction (singular value = 159.35, $P < 0.002$, interaction LV, Fig. 4, see Table 2 for a list of local maxima). The correlation of the brain scores with the seed voxel was negative for auditory comparison and positive for auditory temporal sequencing, whereas the pattern was reversed for the visual conditions (i.e., positive for visual comparison and negative for visual temporal sequencing). The singular image showed dominant positive weights in left superior temporal gyrus (BA 22), left frontal operculum, and more dorsally in superior bilateral parietal lobe (BA 40/7). Dominant negative weights were observed in several areas of occipital cortices, extending from ventral to middle and dorsomedial locations, and right anterior prefrontal gyrus (BA 9). A better appreciation for the nature of this interaction can be obtained by viewing the correlation between the seed voxel and selected locations from the singular image. Figure 5*A* shows the correlation profile for the left superior temporal cortex region with the seed. For the auditory tasks, the correlation profile shows a strong differentiation at lag 2, with auditory comparison showing a negative correlation and auditory temporal sequencing a positive correlation with the seed voxel. The visual tasks differentiate at the same lag, with visual comparison showing a positive correlation and visual temporal sequencing a negative correlation, but the difference was more sustained across subsequent lags. The correlation profile for the anterior PFC voxel is shown in Figure 5*B*. Here the 2 modalities show a different profile of differentiation, both early in lag 1, and then reversing later in lag 6. The maximum bootstrap ratio for this prefrontal voxel was at lag 6, suggesting that the most robust differentiation occurred at that lag.

The second LV showed a task main effect (singular value = 152.44, $P < 0.016$, task demands LV, Fig. 6, see Table 2 for a list of local maxima), with positive correlations for temporal sequencing tasks and negative for comparison tasks. The confidence interval was larger for visual temporal sequencing relative to other tasks, suggesting it was somewhat less stably represented, but the 95% interval did not cross zero. The dominant positive saliences, indicating a more positive correlation in temporal sequencing tasks, were observed in ventromedial PFC (BA 8 and 10) in early lags, and later lags showed strong weights for middle temporal gyrus (BA 21, 22,

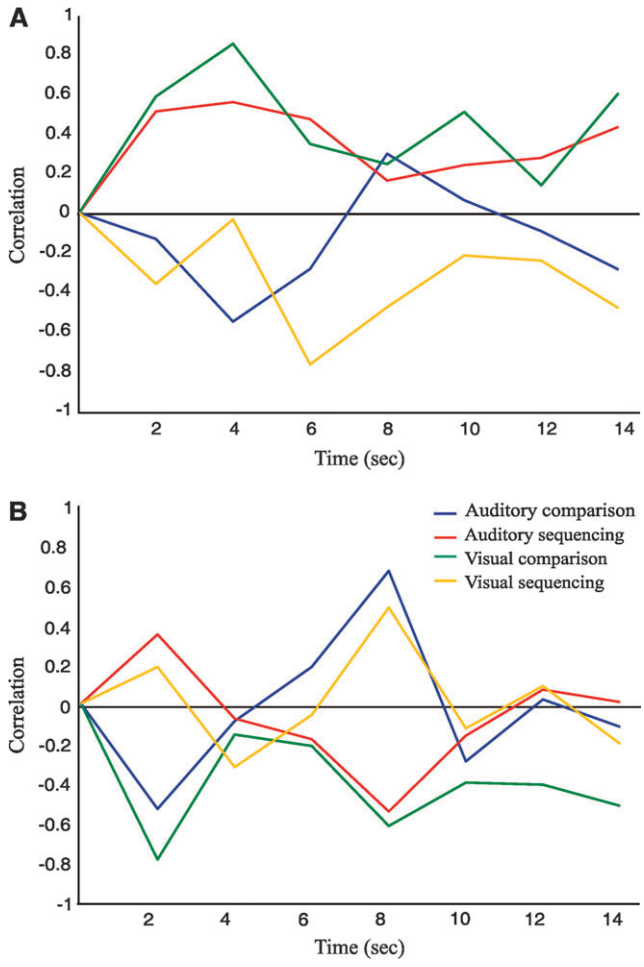

Figure 5. Correlation profiles for selected voxels identified in the interaction LV as shown in Figure 4. Correlations are plotted across the time window from stimulus onset ($T = 0$). (*A*) The correlation for left superior temporal cortex (BA 21, MNI template coordinates: $x = -60$, $y = -48$, $z = 0$) and panel B shows medial PFC (BA 10, MNI template coordinates: $x = 16$, $y = 64$, $z = 4$).

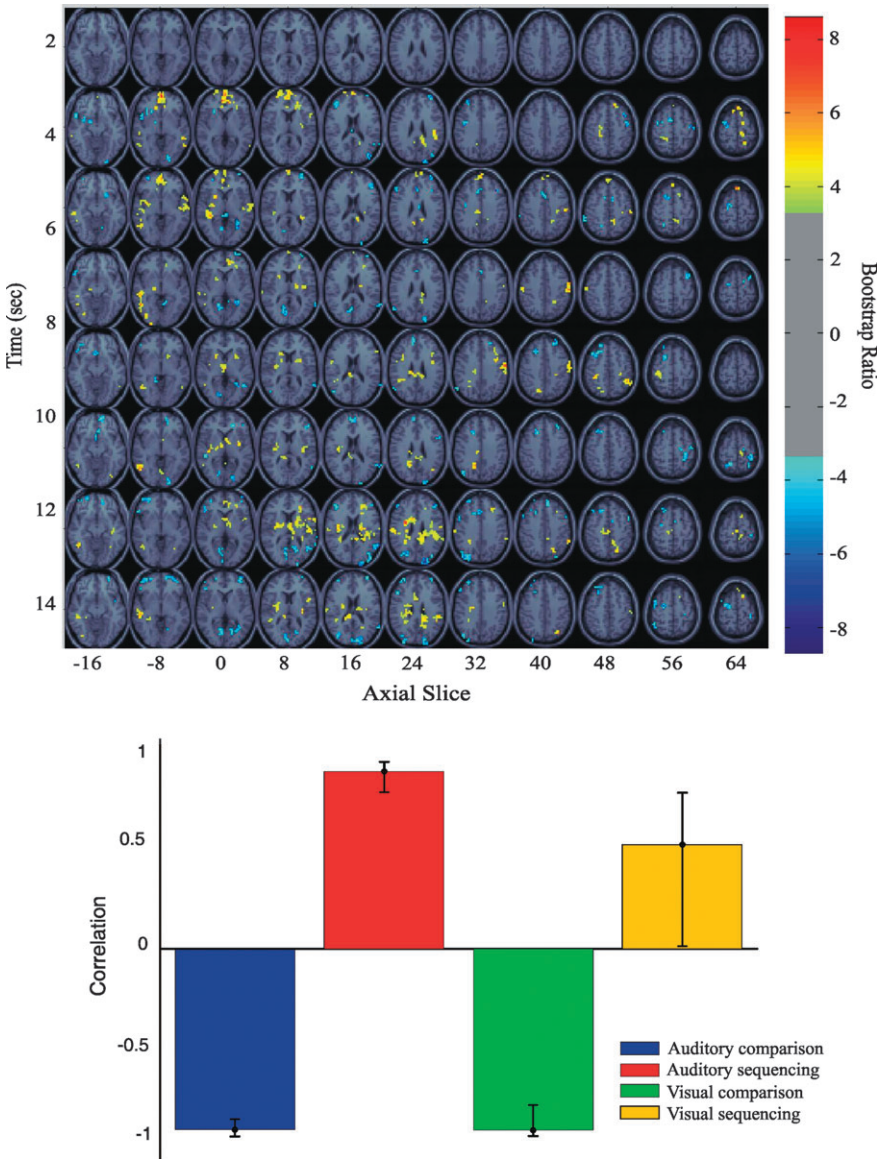

Figure 6. Singular image (top) and correlation between brain scores and the BA 47 seed voxel for the task demands LV from seed PLS. The singular image identifies peak voxels showing a different pattern of correlations with the BA 47 voxel across tasks. The correlation bar graph captures the task-dependent changes in the correlation with the seed voxel of the areas identified in the singular image. The error bars indicate the 95% confidence interval derived from bootstrap estimation.

and 37) and thalamus. Negative saliences, indicating relatively more negative correlations for the comparison tasks, were concentrated on dorsolateral and anterior prefrontal gyrus (BA 9), and occipitoparietal cortices (BA 7 and 19). Representative correlation profiles for maxima from the singular image are presented in Figure 7. The profile for the ventromedial prefrontal region (Fig. 7*A*) shows a strong differentiation between comparison and temporal sequencing at lags 1 and 2, albeit somewhat less for visual comparison as might be anticipated from the lower overall correlation for this condition. The profile for the occipitoparietal region (Fig. 7*B*) shows a more sustained differentiation beginning at lag 1 and extending across the remaining temporal window.

Discussion

We examined the effect of input modality and task demands on neural network organization for simple working memory tasks. Task PLS identified activation patterns that independently map onto modality and task demands. Analysis of functional connectivity (seed PLS) suggested these activity patterns interact.

We used task PLS to identify spatial patterns of brain activity that represent the association between brain images and experimental design. The first significant task PLS LV suggests that functional network organization varies with modality not only in temporal and occipital cortex, but also in prefrontal and parietal cortex. The finding that there are modality-specific areas outside conventional sensory cortices is consistent with previous literature. For example, Bushara et al. (1999) measured brain activity with PET while participants performed auditory and visual spatial localization tasks. They found modality-specific areas in the superior parietal lobule, middle temporal and lateral PFC. Crottaz-Herbette et al. (2004) used fMRI to explore modality-based differences in a verbal and written numbers in a working memory task. They found

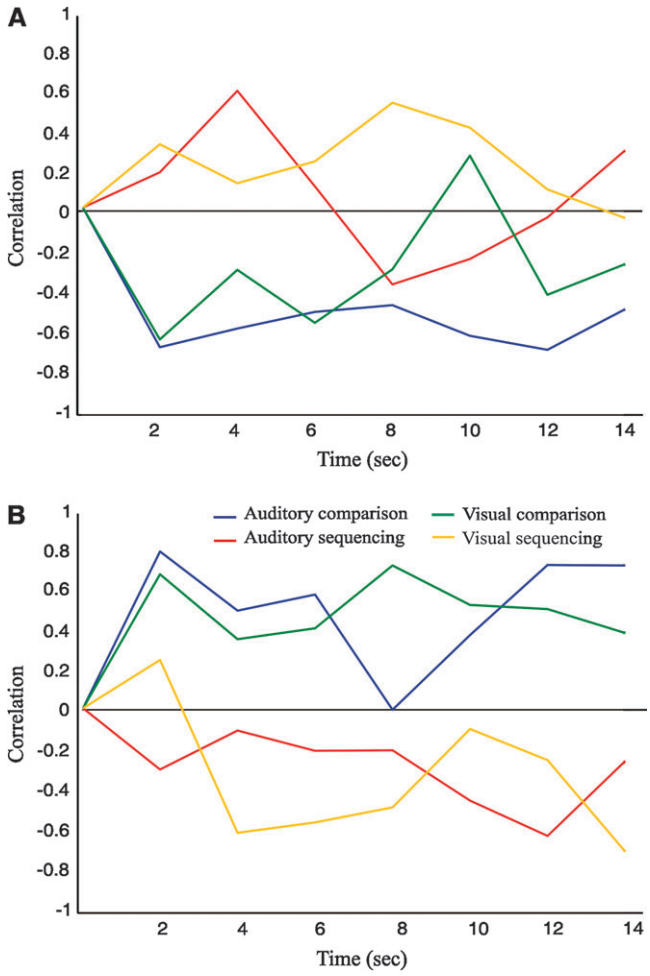

Figure 7. Correlation profiles for selected voxels identified in from the task demands LV as shown in Figure 6. Correlations are plotted across the time window from stimulus onset ($T = 0$). (*A*) The correlation for ventromedial PFC (BA 10, MNI template coordinates: $x = 0$, $y = 60$, $z = -4$); and (*B*) occipitoparietal cortex (BA 19, MNI template coordinates: $x = 16$, $y = -94$, $z = 24$).

modality-based differences in the left posterior parietal cortex and left dorsolateral PFC. In nonhuman primates, Romanski and Goldman-Rakic (2002) found neurons in the ventral PFC that showed selective responses to auditory or to visual stimuli. Finally, both the auditory and visual system are organized into 2 domain-dependent processing streams (Cavada and Goldman-Rakic 1993; Distler et al. 1993; Rauschecker et al. 1997; Belin and Zatorre 2000; Romanski et al. 2000; Alain et al. 2001). Modality of input seems to interact with these processing streams in that activations following auditory input have different anatomical locations outside the sensory cortices as compared to activations following visual input.

The second significant task PLS LV suggests that network organization varies with experimental versus control tasks in ventrolateral and medial PFC, temporal pole, and parietal cortex. Of note is the finding is that there is relatively more frontal involvement (including left ACC, left medial PFC, and left dorsolateral PFC) during the control tasks than during the experimental tasks. The spatial pattern of activation during the control tasks is consistent with the default mode literature, which suggests ventral ACC and medial PFC are involved in a network that is active during conditions with no particular external focus, and reduced during the performance of externally cued tasks (Raichle et al. 2001). Although our control tasks involve minimal cognitive demand, they do not represent a true resting state because they involve externally cued events. However, Greicius et al. (2003) showed that the default mode network only is minimally disrupted by sensory processing tasks with limited cognitive demand. They looked at the functional connectivity of ventral ACC and posterior cingulate during a visual processing task and during rest. They found that that functional connectivity patterns were very similar in both conditions: virtually identical for ventral ACC, and very similar but more inclusive for posterior cingulate in the visual processing task. The added regions included left dorsolateral PFC, which also shows up as a node in the network identified in the current experiment for the control tasks.

The task PLS showed no reliable large-scale activity patterns to suggest an interaction between modality and task demands. However, to do the tasks, both networks must be engaged. A previous study of functional connectivity (Nyberg et al. 2000) suggests that it is possible that the convergence of networks could be revealed by their interactions. Additionally, in a previously published analysis of the data used in the current study, we performed behavioral PLS to examine the neural patterns that capture the optimal association between brain images and reaction time (Protzner and McIntosh, 2007). We found a significant interaction between stimulus modality and task demands in terms of brain–behavior correlations. We used seed PLS to see if there exists an interaction between modality and task demands in terms of functional connectivity. Here, we were interested in whether correlations between the PFC and the rest of the brain changed across tasks. Within the PFC, we chose our ROI statistically. We used the voxel that most stably differentiated experimental from control tasks, as identified in the task demands LV from the task PLS. This voxel was located in right ventral PFC, in BA 47. As mentioned in the introduction, ventral PFC tends to be recruited for maintenance operations (Courtney et al. 1998; D'Esposito et al. 1998; Wager and Smith 2003). Additionally, a review paper by Petrides (2005) and a meta-analysis by Wager and Smith (2003) suggest that BA 47 is more active when participants make active decisions about information maintained in working memory. These are common processing demands for both the temporal sequencing and comparison tasks.

The seed PLS revealed 2 significant LVs regarding BA 47 functional connectivity: a task main effect, and an interaction between stimulus modality and task demands. The other 2 potential patterns of functional connectivity—one showing modality main effect and the other a common task-independent pattern—were not statistically reliable. The task main effect identified modality-independent task differences in functional connectivity. Regions that showed a positive correlation with BA 47 during temporal sequencing were ventromedial PFC, superior temporal cortices, thalamus and basal ganglia. Regions that showed positive correlations during comparison involved more dorsal and lateral PFC regions, dorsal occipital, and parietal cortices. Such differences in functional connectivity patterns could reflect the higher demands in terms of attention and the need to manipulate stimuli in the comparison task. The greater attentional demands could be inferred from the behavioral data wherein reaction times were longer for comparison task independent of stimulus modality.

The second pattern of BA 47 functional connectivity showed an interaction between task and stimulus modality, and was active simultaneously with the task main effect. Some prefrontal regions were engaged in this pattern, but more dominant contributions came from temporal and occipital cortices, distinct from primary sensory areas (e.g., lateral occipital, posterior and anterior superior temporal cortices). For example, as shown in Figure 7*B*, the nature of this interaction was such that the occipitoparietal cortex showed a similar absolute magnitude of functional connectivity with the BA 47 voxel in all tasks, but the sign of the functional connection varied with stimulus modality and task. Importantly, temporal and occipital regions showed nonzero functional connectivity in all conditions, rather than showing a zero connectivity in one modality and nonzero in the other. The interaction represents the modulation of functional connectivity (identified in the task main effect) that is dependent on performing the task in a particular stimulus modality.

Considered together, the 2 patterns of functional connectivity derived from the seed PLS suggest that the same cognitive processes are performed by different functional networks when the modality of input changes. Therefore, our ventrolateral PFC seed showed contextually dependent changes in functional connectivity in relation to the modality of input despite similar cognitive demands. This observation supports the idea that cognitive processes are a supported by reentrant interactions at local and distal levels.

Funding

Canadian Institutes of Health Research (CIHR), JS McDonnell Foundation, and Natural Sciences and Engineering Research Council grants to A.R.M.; and CIHR Doctoral Research Award to A.B.P.

Notes

Conflict of Interest: None declared.

Address correspondence to Andrea B. Protzner, Department of Neuropsychology, Toronto Western Hospital & Research Institute, 399 Bathurst Street, Rm. 4F-409, Toronto, ON M5T 2S8, Canada. Email: protzner@uhnres.utoronto.ca.

References

Alain C, Arnott SR, Hevenor S, Graham S, Grady CL. 2001. "What" and "where" in the human auditory system. Proc Natl Acad Sci USA. 98:12301–12306.

Belin P, Zatorre RJ. 2000. 'What', 'where' and 'how' in auditory cortex. Nat Neurosci. 3:965–966.

Bressler SL, McIntosh AR. 2007. The role of neural context in large-scale neurocognitive network operations. In: Jirsa V, McIntosh AR, editors. Handbook of brain connectivity. New York: Springer. p. 403–420.

Bushara KO, Weeks RA, Ishii K, Catalan MJ, Tian B, Rauschecker JP, Hallett M. 1999. Modality-specific frontal and parietal areas for auditory and visual spatial localization in humans. Nat Neurosci. 2:759–766.

Cabeza R, Nyberg L. 2000. Imaging cognition II: an empirical review of 275 PET and fMRI studies. J Cogn Neurosci. 12:1–47.

Cavada C, Goldman-Rakic PS. 1993. Multiple visual areas in the posterior parietal cortex of primates. Prog Brain Res. 95:123–137.

Corbetta M. 1998. Frontoparietal cortical networks for directing attention and the eye to visual locations: identical, independent, or overlapping neural systems? Proc Natl Acad Sci USA. 95:831–838.

Courtney SM, Petit L, Haxby JV, Ungerleider LG. 1998. The role of prefrontal cortex in working memory: examining the contents of consciousness. Philos Trans R Soc Lond B Biol Sci. 353:1819–1828.

Cox RW. 1996. AFNI: software for analysis and visualization of functional magnetic resonance neuroimages. Comput Biomed Res. 29:162–173.

Crottaz-Herbette S, Anagnoson RT, Menon V. 2004. Modality effects in verbal working memory: differential prefrontal and parietal responses to auditory and visual stimuli. Neuroimage. 21:340–351.

D'Esposito M, Aguirre GK, Zarahn E, Ballard D, Shin RK, Lease J. 1998. Functional MRI studies of spatial and nonspatial working memory. Brain Res Cogn Brain Res. 7:1–13.

Distler C, Boussaoud D, Desimone R, Ungerleider LG. 1993. Cortical connections of inferior temporal area TEO in macaque monkeys. J Comp Neurol. 334:125–150.

Friston KJ. 1994. Functional and effective connectivity: a synthesis. Hum Brain Mapp. 2:56–78.

Friston KJ, Ashburner J, Frith CD, Pline J-B, Heather JD, Frackowiak RSJ. 1995. Spatial registration and normalization of images. Hum Brain Mapp. 2:165–189.

Friston KJ, Buechel C, Fink GR, Morris J, Rolls E, Dolan RJ. 1997. Psychophysiological and modulatory interactions in neuroimaging. Neuroimage. 6:218–229.

Fuster JM. 1997. Network memory. Trends Neurosci. 20:451–459.

Grady CL. 1999. Neuroimaging and activation of the frontal lobes. In: Miller BL, Cummings JL, editors. The human frontal lobes: function and disorders. New York: Guilford Press. p. 196–230.

Greicius MD, Krasnow B, Reiss AL, Menon V. 2003. Functional connectivity in the resting brain: a network analysis of the default mode hypothesis. Proc Natl Acad Sci USA. 100:253–258.

Horwitz B, Grady CL, Haxby JV, Schapiro MB, Rapoport SI, Ungerleider LG, Mishkin M. 1992. Functional associations among human posterior extrastriate brain regions during object and spatial vision. J Cogn Neurosci. 4:311–322.

Lenartowicz A, McIntosh AR. 2005. The role of anterior cingulate cortex in working memory is shaped by functional connectivity. J Cogn Neurosci. 17:1026–1042.

McIntosh AR, Chau WK, Protzner AB. 2004. Spatiotemporal analysis of event-related fMRI data using partial least squares. Neuroimage. 23:764–775.

McIntosh AR, Lobaugh NJ. 2004. Partial least squares analysis of neuroimaging data: applications and advances. Neuroimage. 23(Suppl. 1):S250–S263.

McIntosh AR, Nyberg L, Bookstein FL, Tulving E. 1997. Differential functional connectivity of prefrontal and medial temporal cortices during episodic memory retrieval. Hum Brain Mapp. 5:323–327.

McIntosh AR, Rajah MN, Lobaugh NJ. 2003. Functional connectivity of the medial temporal lobe relates to learning and awareness. J Neurosci. 23:6520–6528.

Nyberg L. 1998. Mapping episodic memory. Behav Brain Res. 90:107–114.

Nyberg L, Habib R, Tulving E, Cabeza R, Houle S, Persson J, McIntosh AR. 2000. Large scale neurocognitive networks underlying episodic memory. J Cogn Neurosci. 12:163–173.

Owen AA, Evans AC, Petrides M. 1996. Evidence for a two-stage model of spatial working memory processing within the lateral frontal cortex: a positron emission tomography study. Cereb Cortex. 6:31–38.

Petrides M. 1994. Frontal lobes and working memory: Evidence from investigations of the effects of cortical excisions in nonhuman primates. In: Boller F, Grafman J, editors. Handbook of neuropsychology. New York: Elsevier Science B.V. p. 59–82.

Petrides M. 2005. Lateral prefrontal cortex: architectonic and functional organization. Philos Trans R Soc Lond B Biol Sci. 360:781–95.

Press WH, Flannery BP, Teukolsky SA, Vetterling WT. 1989. Numerical recipes in Pascal: the art of scientific computing. New York: Cambridge University Press.

Protzner AB, McIntosh AR. 2007. The interplay of stimulus modality and response latency in neural network organization for simple working memory tasks. J Neurosci. 27:3187–3197.

Raichle ME, MacLeod AM, Snyder AZ, Powers WJ, Gusnard DA, Shulman GL. 2001. A default mode of brain function. Proc Natl Acad Sci USA. 98:676–682.

Rauschecker JP, Tian B, Pons T, Mishkin M. 1997. Serial and parallel processing in rhesus monkey auditory cortex. J Comp Neurol. 382:89–103.

Romanski LM, Goldman-Rakic PS. 2002. An auditory domain in primate prefrontal cortex. Nat Neurosci. 5:15–16.

Romanski LM, Tian B, Fritz JB, Mishkin M, Goldman-Rakic PS, Rauschecker JP. 2000. Reply to "What', 'where' and 'how' in auditory cortex'. Nat Neurosci. 3:966.

Rushworth MF, Buckley MJ, Gough PM, Alexander IH, Kyriazis D, McDonald KR, Passingham RE. 2005. Attentional selection and action selection in the ventral and orbital prefrontal cortex. J Neurosci. 25:11628–11636.

Stephan KE, Marshall JC, Friston KJ, Rowe JB, Ritzl A, Zilles K, Fink GR. 2003. Lateralized cognitive processes and lateralized task control in the human brain. Science. 301:384–386.

Stuss DT, Shallice T, Alexander MP, Picton TW. 1995. A multidisciplinary approach to anterior attentional functions. In: Grafman J, Holyoak KJ, Boller F, editors. Structure and function of the human prefrontal cortex. New York: Annals of the New York Academy of Sciences. p. 191–211.

Talairach J, Tournoux P. 1988. Co-planar stereotaxic atlas of the human brain. New York: Thieme Medical Publishers.

Visscher KM, Kaplan E, Kahana MJ, Sekuler R. 2007. Auditory short-term memory behaves like visual short-term memory. PLoS Biol. 5:e56.

Wager TD, Smith EE. 2003. Neuroimaging studies of working memory: a meta-analysis. Cogn Affect Behav Neurosci. 3:255–274.

Watson AB, Pelli DG. 1983. QUEST: a Bayesian adaptive psychometric method. Percept Psychophys. 33:113–120.

Wilson FA, Scalaidhe SP, Goldman-Rakic PS. 1993. Dissociation of object and spatial processing domains in primate prefrontal cortex. Science. 260:1955–1958.